Supplementary data to 'Noisy cell growth rate leads to fluctuating protein concentration in bacteria'

Saburo Tsuru *et al*

Table of contents

Supplementary text

1. Stochastic model of protein concentration

1.1. Langevin equation for noise in cell growth rate

Considering the noise in the cell growth rate, we propose the following Langevin equation:

$$\frac{\mathrm{d}x}{\mathrm{d}t} = k_x - \left(\mu_0 + \sqrt{D_\mu}\eta_\mu(t)\right)x + \sqrt{b\mu_0\langle x\rangle}\eta_{x,\mathrm{int}}(t) + \langle x\rangle\sqrt{c'\mu_0}\eta_{\mathrm{ext}}(t) \quad \text{(S1.1)}$$

$$\left\langle \eta_\mu(t)\right\rangle = 0 \quad \text{(S1.2)}$$

, where $\eta_\mu(t)$ and D_μ (h^{-1}) represent noise in the cell growth rate and its diffusion coefficient, respectively. Because noise in the cell growth rate influences the dynamics of protein concentration in a multiplicative manner, $\sqrt{D_\mu}\eta_\mu(t)x$, similar to the unspecified extrinsic noise, $\langle x\rangle\sqrt{c'\mu_0}\eta_{\mathrm{ext}}(t)$, a high protein concentration can cause noise large enough to form a constant fluctuation. In this case, the coefficient of extrinsic noise c' represents the summed contributions of sources other than noise in the cell growth rate. According to this theoretical feature, noise in the cell growth rate can be categorized as extrinsic noise. To elucidate the contribution of cell growth rate to protein concentration, noise in the cell growth rate was further investigated by simplifying equation (S1.1) as follows:

$$\frac{\mathrm{d}x}{\mathrm{d}t} = k_x - \left(\mu_0 + \sqrt{D_\mu}\eta_\mu(t)\right)x \quad \text{(S2)}$$

Fast and slow time dependency of $\eta_\mu(t)$ was considered in the evaluation of fluctuation in protein concentration (CV_x) using the white and slow noise limits, respectively. The two approaches ultimately resulted in equivalent conclusions for a steady state.

1.2. Slow noise limit

Cell growth rate at a steady state was studied by the following simple static theoretical procedure, known as the slow noise limit. First, we assumed that cell growth rate remains

constant within a generation but fluctuates at the time of every cell division. The Langevin equation for the *i*th cell or the *i*th generation can be transcribed as follows:

$$\frac{\mathrm{d}x_i(t)}{\mathrm{d}t} = k_x - \left(\mu_0 + \sqrt{D_\mu}\eta_{\mu_i}(t)\right)x_i(t) \tag{S3}$$

Second, cell growth rate is constant for the *i*th cell or the *i*th generation but varies among individual cells or generations:

$$\mu_0 + \sqrt{D_\mu}\eta_{\mu_i}(t) = \mu_i \tag{S4}$$

At a steady state, protein concentration of the *i*th cell or the *i*th generation can be calculated from equations (S3) and (S4).

$$x_i = \frac{k_x}{\mu_i} \tag{S5}$$

Evidently, protein concentration is inversely proportional to cell growth rate.

In addition, the cell growth rate shows a Gaussian distribution $\hat{P}(\mu_i)$ (equation S6) is presumed, according to the similar distribution observed in the microscopic experiments (figure 5(c)).

$$\hat{P}(\mu_i) = \frac{1}{\sqrt{2\pi\sigma_\mu^2}}\exp\left[-\frac{(\mu_i - \mu_0)^2}{2\sigma_\mu^2}\right] \tag{S6}$$

, where μ_0 and σ_μ^2 represent the average cell growth rate and variance, respectively. The CV_μ of the distribution is $\frac{\sigma_\mu}{\mu_0}$, which was observed to be 13% in our experiments (figure 5).

The steady-state distribution of protein concentration, $P(x_i)$, was then constructed by combining equations (S5) and (S6):

$$P(x_i) = \hat{P}(\mu_i)\frac{\mathrm{d}\mu_i}{\mathrm{d}x_i} = \frac{k_x}{{x_i}^2}\frac{1}{\sqrt{2\pi\sigma_\mu^2}}\exp\left[-\frac{\left(\frac{k_x}{x_i} - \mu_0\right)^2}{2\sigma_\mu^2}\right] \tag{S7}$$

, where $\frac{dx_i}{d\mu_i}$ was calculated from equation (S5). The distribution of protein concentration was numerically reconstructed from the only noise in the cell growth rate using equation (S7) with experimentally determined parameters: 0.11 a.u. for k_x, 0.35 h^{-1} for μ_0 and 0.046 h^{-1} for σ_μ (figure 6). The distribution showed a fluctuation (CV_x) of 14%, independent of protein concentration k_x, as schematically interpreted in figure 6. The distribution of cell growth rate is inversely transformed into the distribution of protein concentration (figure 6, arrows).

1.3. Fast (white) noise limit

On the other hand, cell growth rate at a steady state possibly fluctuates frequently within a generation, which can be considered as white noise.

$$\left\langle \eta_\mu(t)\eta_\mu(t') \right\rangle = 2\delta(t-t') \tag{S8}$$

Here, noise in cell growth rate is charged with $\sqrt{\frac{D_\mu}{\ln[2]\mu_0}}$ without relaxation and its corresponding value is CV_μ, the value of which was 13% from microscopic observation. Assigning 0.35 h^{-1} to μ_0, we obtained D_μ as 0.0018 h^{-1}. We transform the Langevin model (equation S3) to the Fokker-Planck equation to determine the dynamics of the distribution [9].

$$\frac{\partial P(x,t)}{\partial t} = \frac{\partial}{\partial x}\left[\left(\mu_0 - D_\mu\right)\left(x - \frac{k_x}{\mu_0 - D_\mu} \right) P(x,t) \right] + \frac{\partial^2}{\partial x^2}\left[D_\mu x^2 P(x,t) \right] \tag{S9}$$

The steady-state distribution is given as follows (figure S1, broken line):

$$P(x) = \frac{C}{x^{1+\frac{\mu_0}{D_\mu}}} \exp\left[-\frac{k_x}{xD_\mu} \right] \tag{S10}$$

Temporal changes in statistical moments are calculated as follows:

$$\frac{\mathrm{d}\langle x\rangle}{\mathrm{d}t} = -\left(\mu_0 - D_\mu\right)\left(\langle x\rangle - \frac{k_x}{\mu_0 - D_\mu}\right) \tag{S11.1}$$

$$\frac{\mathrm{d}\left\langle x^2\right\rangle}{\mathrm{d}t} = -2\left(\mu_0 - 2D_\mu\right)\left\langle x^2\right\rangle + 2k_x\langle x\rangle \tag{S11.2}$$

, where $\langle x\rangle = \int_{-\infty}^{\infty} xP(x,t)\mathrm{d}x$ and $\left\langle x^2\right\rangle = \int_{-\infty}^{\infty} x^2P(x,t)\mathrm{d}x$.

The solutions at a steady state are solved analytically as follows:

$$\langle x\rangle = \frac{k_x}{\mu_0 - D_\mu} \tag{S12.1}$$

$$\left\langle x^2\right\rangle = \frac{k_x\langle x\rangle}{\mu_0 - 2D_\mu} \tag{S12.2}$$

The CV_μ of protein concentration at a steady state is solved as follows:

$$CV_x = \frac{\sigma_x}{\langle x\rangle} = \frac{\sqrt{\left\langle x^2\right\rangle - \langle x\rangle^2}}{\langle x\rangle} = \sqrt{\frac{D_\mu}{\mu_0 - 2D_\mu}} \tag{S13}$$

It is implied that the *CV* of protein concentration remains constant regardless of its mean. We plotted the distribution of protein concentration using equation (S13) with experimentally determined parameters: 0.11 a.u. for k_x, 0.35 h^{-1} for μ_0 and 0.046 h^{-1} for σ_μ (figure S1). The *CV* of the protein concentration turned to be 7.4%, which was 53% of that determined using the slow noise limit. Compared with the slow noise limit, the white noise limit makes a slightly smaller contribution to the fluctuation in protein concentration. Nevertheless, it does not change the large contribution of noise in cell growth rate to the fluctuation in cellular protein concentration at dozens of percent of total extrinsic noise (figure 7(a) and (b)).

2. Contribution of intrinsic noise to fluctuation in GFP concentration: correlation analysis

2.1 Theoretical process

We evaluated the intrinsic noise of GFP from the correlation between GFP and RFP concentrations [4]. We devised a theoretical procedure to extract the incoherent component (intrinsic noise) between GFP and RFP in the genetic circuit. As GFP was downstream of RFP, the fluctuation of RFP could be transmitted to that of GFP [8]. However, the propagation of noise, including transmitted noises (intrinsic and extrinsic), from upstream to downstream, was negligible owing to the full induction by IPTG [8]. As shown in equation (A1), Langevin equations for cellular concentration of GFP (x) and for RFP (y) are formulated in an identical fashion as follows:

$$\frac{\mathrm{d}x}{\mathrm{d}t} = k_x - \mu_0 x + \sqrt{D_{x,\mathrm{int}}}\eta_{x,\mathrm{int}}(t) + \sqrt{D_{x,\mathrm{ext}}}\eta_{\mathrm{ext}}(t) \quad \text{(S14.1)}$$

$$\frac{\mathrm{d}y}{\mathrm{d}t} = k_y - \mu_0 y + \sqrt{D_{y,\mathrm{int}}}\eta_{y,\mathrm{int}}(t) + \sqrt{D_{y,\mathrm{ext}}}\eta_{\mathrm{ext}}(t) \quad \text{(S14.2)}$$

, where $\eta_{x,\mathrm{int}}(t)$ and $\eta_{y,\mathrm{int}}(t)$ represent intrinsic noise (incoherent component) of GFP and RFP, respectively $\eta_{\mathrm{ext}}(t)$ and represents extrinsic noise (coherent component) shared by both proteins. The white noise limit for each noise and the diffusion constant are set similarly, as described previously:

$$\left\langle \eta_j(t) \right\rangle = 0 \quad \text{(S15.1)}$$

$$\left\langle \eta_j(t)\eta_j(t') \right\rangle = 2\delta(t-t') \;\; j \in \mathrm{int}, \mathrm{ext} \quad \text{(S15.2)}$$

$$D_{l,\mathrm{int}} = b\mu_0\langle l \rangle \quad \text{(S16.1)}$$

$$D_{l,\mathrm{ext}} = c\mu_0\langle l \rangle^2 \;\; l \in x, y \quad \text{(S16.2)}$$

Substituting equations (S16.1) and (S16.2) in equations (S14.1) and (S14.2) results in the following equations:

$$\frac{\mathrm{d}x}{\mathrm{d}t} = k_x - \mu_0 x + \sqrt{b\mu_0\langle x \rangle}\eta_{x,\mathrm{int}}(t) + \langle x \rangle\sqrt{c\mu_0}\eta_{\mathrm{ext}}(t) \quad \text{(S17.1)}$$

$$\frac{\mathrm{d}y}{\mathrm{d}t} = k_y - \mu_0 y + \sqrt{b\mu_0\langle y \rangle}\eta_{y,\mathrm{int}}(t) + \langle y \rangle\sqrt{c\mu_0}\eta_{\mathrm{ext}}(t) \quad \text{(S17.2)}$$

, where the contribution from intrinsic noise to *CV* is calculated as follows:

$$CV_{l,\text{int}} = \sqrt{\frac{b}{\langle l \rangle}} \quad l \in x, y \tag{S18}$$

The protein concentration is normalized by its average:

$$\frac{\mathrm{d}}{\mathrm{d}t}\frac{x}{\langle x \rangle} = \frac{k_x}{\langle x \rangle} - \mu_0 \frac{x}{\langle x \rangle} + \sqrt{\frac{b\mu_0}{\langle x \rangle}}\eta_{x,\text{int}}(t) + \sqrt{c\mu_0}\eta_{\text{ext}}(t) \tag{S19.1}$$

$$\frac{\mathrm{d}}{\mathrm{d}t}\frac{y}{\langle y \rangle} = \frac{k_y}{\langle y \rangle} - \mu_0 \frac{y}{\langle y \rangle} + \sqrt{\frac{b\mu_0}{\langle y \rangle}}\eta_{y,\text{int}}(t) + \sqrt{c\mu_0}\eta_{\text{ext}}(t) \tag{S19.2}$$

Subtracting equation (S19.2) from equation (S19.1) leads to the elimination of the coherent component (extrinsic noise) and extraction of the incoherent component:

$$\frac{\mathrm{d}z}{\mathrm{d}t} = k_z - \mu_0 z + \sqrt{\frac{b\mu_0}{\langle x \rangle}}\eta_{x,\text{int}}(t) - \sqrt{\frac{b\mu_0}{\langle y \rangle}}\eta_{y,\text{int}}(t) \tag{S20}$$

, where

$$z = \frac{x}{\langle x \rangle} - \frac{y}{\langle y \rangle} \tag{S21.1}$$

$$k_z = \frac{k_x}{\langle x \rangle} - \frac{k_y}{\langle y \rangle} \tag{S21.2}$$

The standard deviation of z is calculated:

$$\sigma_z = \sqrt{b\left(\frac{1}{\langle x \rangle} + \frac{1}{\langle y \rangle}\right)} \tag{S22}$$

Employing the experimental data, equation (S22) was used to calculate the coefficient b, which is used to estimate the contribution of intrinsic noise to GFP (equation (S18), figure S4).

2.2. Estimation of intrinsic noise

The normalized concentrations of GFP and RFP were plotted (figure S2). These data show that a higher doxycycline hydrochloride (Dox) concentration led to a better correlation between GFP

and RFP (figure S2), which indicates the decreasing contribution of the incoherent component, intrinsic noise, with increasing GFP concentrations. The distribution of points perpendicular to the diagonal line corresponds to the incoherent component, the fluctuation of z (figure S3(a)). The standard deviations of the distributions were calculated (figure S3(b)). Applying equation (S22) to each standard deviation resulted in the coefficient b (figure S3(c)), which exhibited an average of 0.013 (a.u.). Using equation (S18), the intrinsic noise causing the fluctuation in GFP concentration was constructed (figure S4). The result (slope) was consistent with that in the main text (broken line in figure 7), which verified our estimation of intrinsic noise.

3. Classification of extrinsic noise

Although the many origins of extrinsic noise have not yet been identified completely, extrinsic noise has been systematically interpreted by dividing it into two categories: transmitted noise from upstream genes and global noise affecting all genes [6, 8]. The extrinsic noise of GFP consists of transmitted noises from RFP and global noise. Correspondingly, the extrinsic noise of RFP comprises transmitted noises from LacI and global noise. The degree of transmitted noise depends on the susceptibility of the network architecture, i.e. how much the expression of the downstream gene changes with alterations in the expression level of upstream gene [1, 3, 8]. If the susceptibility of the downstream gene to the upstream gene is strong enough, the transmitted noise from the upstream gene is then dominant over extrinsic noise [1, 8]. Protein concentrations of the upstream and downstream genes would exhibit a negative correlation, as the upstream gene represses the downstream gene because of the structure of the genetic circuit [8].

On the other hand, such susceptibility can be converted to insensitivity by adding IPTG at a full induction level. Consequently, the global noise serves as the leading factor causing fluctuation in protein concentration. In this case, the two protein concentrations should be positively correlated, regardless of the network architecture [8]. Because the purpose is to

isolate the potential source of global noise, IPTG was supplied at a full induction level to prevent the propagation of noise from upstream (RFP) to downstream (GFP), and to reduce the intrinsic noise in RFP expression, which plays a major role in the fluctuation in RFP concentration, to a negligible level. The positive correlation between GFP and RFP demonstrates that the possible transmitted noise from RFP to GFP was small enough to be ignored (figure S2). In addition, the magnitude of extrinsic noise of GFP was approximately equal to that of RFP, irrespective of whether gated or total cells are considered (figures S5 and S6, figure 7(a) and (b)). Taken together, the results indicate that most of the extrinsic noise of GFP and RFP was global noise [8].

4. Derivation of models considering mRNA steps

The deterministic formation of protein concentration including mRNA step is constructed as follows. Cell volume, V, grows exponentially within a single generation, which is learned from the experimental data that the cell length of the rod-shaped *E. coli* cells increases exponentially (figure 5(b)).

$$\frac{dV}{dt} = \mu V \tag{S23}$$

The abundance of biomass (*e. g.* DNA) in a single cell, B, which is essential to produce mRNA or protein, simultaneously increases exponentially, following the enlargement of the cell volume.

$$\frac{dB}{dt} = \mu B \tag{S24}$$

The abundance of mRNA in a single cell, m, is constantly produced from the biomass and degraded in a first-order rate.

$$\frac{dm}{dt} = k_m B - \gamma_m m \tag{S25}$$

, where k_m and γ_m are the rate constants for production and degradation respectively.

Similarly, the abundance of protein in a single cell, p, is produced from mRNA with a constant rate and degraded in a first-order rate.

$$\frac{dp}{dt} = k_p m - \gamma_p p \tag{S26}$$

, where k_p and γ_p are rate constant for production and degradation, respectively.

The dynamics of the concentration of biomass, mRNA, and protein are derived from the above described conditions. The concentration of biomass is constant due to the coupling of biomass to the cell growth.

$$\frac{d}{dt}\left(\frac{B}{V}\right) = \frac{1}{V}\frac{dB}{dt} - \frac{B}{V^2}\frac{dV}{dt} = 0 \tag{S27}$$

The steady concentration of biomass is described as follows.

$$\frac{B}{V} = \frac{B_0}{V_0} \tag{S28}$$

The dynamics of concentration of mRNA and protein are derived as follows.

$$\frac{d}{dt}\left(\frac{m}{V}\right) = \frac{1}{V}\frac{dm}{dt} - \frac{m}{V^2}\frac{dV}{dt} = k_m\left(\frac{B_0}{V_0}\right) - \left(\gamma_m + \mu\right)\left(\frac{m}{V}\right) \tag{S29}$$

$$\frac{d}{dt}\left(\frac{p}{V}\right) = \frac{1}{V}\frac{dp}{dt} - \frac{p}{V^2}\frac{dV}{dt} = k_p\left(\frac{m}{V}\right) - \left(\gamma_p + \mu\right)\left(\frac{p}{V}\right) \tag{S30}$$

Note that the decay rate of each concentration is characterized not only by the rate constant of degradation but also by that of dilution.

Case 1: long-lived protein synthesized from short-lived mRNA

Lifetime of most proteins in bacterial cells is much longer than a generation time [10, 5]. On the other hand, their mRNAs are unstable and their lifetime is much shorter [2]. These proteins and their mRNAs obey the following rule.

$$\gamma_m >> \mu >> \gamma_p \tag{S31}$$

Under this condition, the mRNA concentration approaches the steady concentration in a fast time scale relative to the protein concentration does. Thus, the equations (S29) and (S30) can be combined as follows.

$$\frac{d}{dt}\left(\frac{m}{V}\right) \approx k_m\left(\frac{B_0}{V_0}\right) - \gamma_m\left(\frac{m}{V}\right) = 0 \tag{S32}$$

, where steady concentration of mRNA is derived as equation (S33).

$$\left.\frac{m}{V}\right|_{st} = \frac{k_m}{\gamma_m}\left(\frac{B_0}{V_0}\right) \tag{S33}$$

The temporal change of protein concentration under the steady state of mRNA concentration is described as follows.

$$\left.\frac{d}{dt}\left(\frac{p}{V}\right)\right|_{\left(\frac{m}{V}\right)_{st}} = k_p\left.\left(\frac{m}{V}\right)\right|_{st} - \mu\left(\frac{p}{V}\right) = k_p\frac{k_m}{\gamma_m}\left(\frac{B_0}{V_0}\right) - \mu\left(\frac{p}{V}\right) \tag{S34}$$

Equation (S34) implies that the production rate is constant when being considered as a single term and the decay rate is determined only by the cell growth rate. Thus, it can be simplified as equation (S35) under the condition of equation (36).

$$\frac{dx}{dt} = \left.\frac{d}{dt}\left(\frac{p}{V}\right)\right|_{\left(\frac{m}{V}\right)_{st}} = k_x - \mu x \tag{S35}$$

$$k_x \equiv k_p\frac{k_m}{\gamma_m}\left(\frac{B_0}{V_0}\right) \tag{S36}$$

It leads to equation (1) in the main text. The verification of the equation is experimentally examined as well in the main text. The steady protein concentration is shown in equation (S37).

$$x_{st} = \left.\left(\frac{p}{V}\right)\right|_{st} = \frac{k_p k_m}{\mu\gamma_m}\left(\frac{B_0}{V_0}\right) = \frac{k_x}{\mu} \tag{S37}$$

Case 2: long-lived protein synthesized from long-lived mRNA

In this case, the degradation rate of protein and mRNA is smaller than the cell growth rate (equation (S38). Thus, temporal change of each concentration can be approximately described as equations (S39) and (S40).

$$\mu >> \gamma_m, \gamma_p \tag{S38}$$

$$\frac{d}{dt}\left(\frac{m}{V}\right) \approx k_m\left(\frac{B_0}{V_0}\right) - \mu\left(\frac{m}{V}\right) \tag{S39}$$

$$\frac{d}{dt}\left(\frac{p}{V}\right) \approx k_p\left(\frac{m}{V}\right) - \mu\left(\frac{p}{V}\right) \tag{S40}$$

This means that the temporal change in protein concentration is more complicated because the time scale of temporal change in mRNA concentration is slow, in turn, leads to a much slower protein step. However, when the steady state and its neighbourhood are considered, equation (S40) can be simplified as follows.

$$\frac{d}{dt}\left(\frac{m}{V}\right) \approx k_m\left(\frac{B_0}{V_0}\right) - \mu\left(\frac{m}{V}\right) = 0 \tag{S41}$$

$$\frac{d}{dt}\left(\frac{p}{V}\right)_{st} \approx k_p\left(\frac{m}{V}\right)\Big|_{st} - \mu\left(\frac{p}{V}\right) \quad (=0) \tag{S42}$$

This equation can be simplified as well as that in case 1.

$$\frac{dx}{dt} = \frac{d}{dt}\left(\frac{p}{V}\right)\Big|_{st} = k_p \frac{k_m}{\mu}\left(\frac{B_0}{V_0}\right) - \mu\left(\frac{p}{V}\right) = k_x - \mu x \tag{S43}$$

, where

$$k_x \equiv k_p \frac{k_m}{\mu}\left(\frac{B_0}{V_0}\right) \tag{S44}$$

Thus, it gives equation (1) as well.

The steady protein concentration is given as equation (S45).

$$x_{st} = \left(\frac{p}{V}\right)\Big|_{st} = \frac{k_p k_m}{\mu^2}\left(\frac{B_0}{V_0}\right) \tag{S45}$$

As shown, the format of maintaining protein concentration at the steady state is captured by equation (1) either in case 1 or 2. Here, production rate (or steady concentration) of protein increases with lifetime of mRNA until it comes close to generation time as shown in equation (S36) and (S44) (or equation (S37) and (S45)). Note that production rate, k_x, estimated in the main text including this effect of the lifetime of mRNA.

Furthermore, mRNA steps play a role in defining the magnitude of intrinsic noise that contributes to the fluctuation of protein concentration [7, 11]. The stochastic model, equation (A1), is from deterministic model, equation (1). Diffusion constant of intrinsic noise is completely interpreted by considering mRNA step as following described. The stochastic model of intrinsic noise in protein concentration is characterized by the expansion of the deterministic equations (S29) and (S30).

$$\frac{d}{dt}\left(\frac{m}{V}\right) = k_m\left(\frac{B_0}{V_0}\right) - \left(\gamma_m + \mu\right)\left(\frac{m}{V}\right) + \eta_{m,\mathrm{int}}(t) \tag{S46}$$

$$\frac{d}{dt}\left(\frac{p}{V}\right) = k_p\left(\frac{m}{V}\right) - \left(\gamma_p + \mu\right)\left(\frac{p}{V}\right) + \eta_{p,\mathrm{int}}(t) \tag{S47}$$

, where $\eta_{m,\mathrm{int}}(t)$ and $\eta_{p,\mathrm{int}}(t)$ represent intrinsic noise in mRNA and protein steps respectively. They are introduced by white noise sources using the following statistics:

$$\left\langle \eta_{i,\mathrm{int}}(t) \right\rangle = 0 \tag{S48}$$

$$\left\langle \eta_{i,\mathrm{int}}(t)\eta_{i,\mathrm{int}}(t') \right\rangle = 2D_{i,\mathrm{int}}\delta(t-t') \tag{S49}$$

$i \in m, p$

, where $D_{i,\mathrm{int}}$ represents the diffusion constant and δ is the Dirac delta function.

The mean mRNA concentration at the steady state is derived from equation (S46).

$$\left\langle \left(\frac{m}{V}\right) \right\rangle_{st} = \frac{k_m}{\gamma_m + \mu} \tag{S50}$$

When the fluctuation is around the steady state as shown in equation (S51), it gives equation (S52).

$$\left(\frac{m}{V}\right) = \left\langle \left(\frac{m}{V}\right) \right\rangle_{st} + \delta\left(\frac{m}{V}\right) \tag{S51}$$

$$\frac{d}{dt}\delta\left(\frac{m}{V}\right) = -(\gamma_m + \mu)\delta\left(\frac{m}{V}\right) + \eta_{m,\mathrm{int}}(t) \tag{S52}.$$

Fourier-transforming of equation (S52) results in equation (S53).

$$\delta\left(\frac{\hat{m}}{V}\right) = \frac{\hat{\eta}_{m,\mathrm{int}}}{\gamma_m + \mu + i\omega} \tag{S53}$$

, where hats denotes variables evaluated in Fourier space.

Note that power specter of white noise gives equation (S54).

$$\left\langle \left|\hat{\eta}_{m,\mathrm{int}}\right|^2 \right\rangle = 2D_{m,\mathrm{int}} \tag{S54}.$$

The steady state variance of mRNA concentration around average is obtained by squaring, averaging and transforming back according to the Wiener-Khinchine theorem.

$$\left\langle \delta\left(\frac{m}{V}\right)^2 \right\rangle = \int \frac{d\omega}{2\pi} \frac{2D_{m,\mathrm{int}}}{(\gamma_m + \mu)^2 + \omega^2} = \frac{D_{m,\mathrm{int}}}{\gamma_m + \mu} \tag{S55}$$

By imposing Poisson statistics as shown in equation (S56) results in equation (S57) and (S58).

$$\left\langle \delta\left(\frac{m}{V}\right)^2 \right\rangle = \left\langle \left(\frac{m}{V}\right) \right\rangle \tag{S56}$$

$$D_{m,\mathrm{int}} = k_m \tag{S57}$$

$$D_{p,\mathrm{int}} = \frac{k_p k_m}{\gamma_m + \mu} \tag{S58}$$

Fluctuation of protein concentration comprising that of mRNA concentration (equation (S51)) around the steady state, as shown in equation (S59), gives equation (S60). The following Fourier-transforming leads to equation (S61) and (S62).

$$\frac{d}{dt}\left(\left\langle\left(\frac{p}{V}\right)\right\rangle_{st}+\delta\left(\frac{p}{V}\right)\right)=k_p\left(\left\langle\left(\frac{m}{V}\right)\right\rangle_{st}+\delta\left(\frac{m}{V}\right)\right)-\left(\gamma_p+\mu\right)\left(\left\langle\left(\frac{p}{V}\right)\right\rangle_{st}+\delta\left(\frac{p}{V}\right)\right)+\eta_{p,\mathrm{int}}(t)$$

(S59)

$$\frac{d}{dt}\delta\left(\frac{p}{V}\right)=k_p\delta\left(\frac{m}{V}\right)-\left(\gamma_p+\mu\right)\delta\left(\frac{p}{V}\right)+\eta_{p,\mathrm{int}}(t) \tag{S60}$$

$$\delta\left(\frac{\hat{p}}{V}\right)=\frac{1}{\gamma_p+\mu+i\omega}\left(\hat{\eta}_{p,\mathrm{int}}+k_p\delta\left(\frac{\hat{m}}{V}\right)\right)=\frac{1}{\gamma_p+\mu+i\omega}\left(\hat{\eta}_{p,\mathrm{int}}+\frac{k_p\hat{\eta}_{m,\mathrm{int}}}{\gamma_m+\mu+i\omega}\right) \tag{S61}$$

$$\left\langle\delta\left(\frac{p}{V}\right)^2\right\rangle=\int\frac{d\omega}{2\pi}\frac{1}{\left(\gamma_p+\mu\right)^2+\omega^2}\left(2D_{p,\mathrm{int}}+\frac{2k_p^2D_{m,\mathrm{int}}}{\left(\gamma_m+\mu\right)^2+\omega^2}\right)=\left\langle\left(\frac{p}{V}\right)\right\rangle\left(1+\frac{k_p}{\gamma_m+\gamma_p+2\mu}\right)$$

(S62).

The relative fluctuation (CV) of protein concentration, which derived from intrinsic noise, is derived as follows, including mRNA step.

$$CV_{x,\mathrm{int}}\equiv\frac{\sigma_p}{\left\langle\left(\frac{p}{V}\right)\right\rangle}\equiv\frac{\sqrt{\left\langle\delta\left(\frac{p}{V}\right)^2\right\rangle}}{\left\langle\left(\frac{p}{V}\right)\right\rangle}=\sqrt{\frac{b}{\left\langle\left(\frac{p}{V}\right)\right\rangle}}=\sqrt{\frac{b}{\langle x\rangle}} \tag{S63}$$

, where

$$b\equiv1+\frac{k_p}{\gamma_m+\gamma_p+2\mu} \tag{S64}.$$

It is identical to the intrinsic contribution described in equation (A5.3) (or equation (S18)) derived from equation (A1). Equation (S64) indicates that magnitude of intrinsic noise increases along with the lifetime of mRNA. Most mRNAs satisfies the condition in equation (S65), which results in equation (S66).

$$\gamma_m>>\mu,\gamma_p \tag{S65}$$

$$b\approx1+\frac{k_p}{\gamma_m}\approx\frac{k_p}{\gamma_m} \tag{S66}.$$

b is called as burst size and represents the number of protein synthesized from a single mRNA during the lifetime of mRNA. Note that magnitude of intrinsic noise, b, estimated in the main text counts this effect of the lifetime of mRNA.

Supplementary references

[1] Becskei A, Kaufmann B B and van Oudenaarden A 2005 Contributions of low molecule number and chromosomal positioning to stochastic gene expression *Nat Genet* **37** 937-44

[2] Bernstein J A, Khodursky A B, Lin P H, Lin-Chao S and Cohen S N 2002 Global analysis of mRNA decay and abundance in Escherichia coli at single-gene resolution using two-color fluorescent DNA microarrays *Proc Natl Acad Sci U S A* **99** 9697-702

[3] Dunlop M J, Cox R S, 3rd, Levine J H, Murray R M and Elowitz M B 2008 Regulatory activity revealed by dynamic correlations in gene expression noise *Nat Genet*

[4] Elowitz M B, Levine A J, Siggia E D and Swain P S 2002 Stochastic gene expression in a single cell *Science* **297** 1183-6

[5] Nath K and Koch A L 1970 Protein degradation in Escherichia coli. I. Measurement of rapidly and slowly decaying components *J Biol Chem* **245** 2889-900

[6] Newman J R, Ghaemmaghami S, Ihmels J, Breslow D K, Noble M, DeRisi J L and Weissman J S 2006 Single-cell proteomic analysis of S. cerevisiae reveals the architecture of biological noise *Nature* **441** 840-6

[7] Ozbudak E M, Thattai M, Kurtser I, Grossman A D and van Oudenaarden A 2002 Regulation of noise in the expression of a single gene *Nat Genet* **31** 69-73

[8] Pedraza J M and van Oudenaarden A 2005 Noise propagation in gene networks *Science* **307** 1965-9

[9] Risken H 1989 The Fokker-Planck Equations *Berlin Hiedelberg New York: Springer*

[10] Rosenfeld N, Elowitz M B and Alon U 2002 Negative autoregulation speeds the response times of transcription networks *J Mol Biol* **323** 785-93

[11] Yu J, Xiao J, Ren X, Lao K and Xie X S 2006 Probing gene expression in live cells, one protein molecule at a time *Science* **311** 1600-3

Supplementary figure legends

Figure S1. Steady-state distributions of white noise limit and slow noise limit. The steady-state distributions obtained from the slow noise limit (equation (S7), solid line) and the white noise limit (equation (S10), broken line) are plotted. The parameters are as follows: k_x = 0.11 a.u., μ_0 = 0.35 h^{-1}, D_μ = 0.0018 h^{-1} and σ_μ^2 = 0.002 h^{-2}, which were calculated from experimental observations (figures 4 and 5). The *CV* values of the distribution are 14% (solid line) and 7.4% (broken line), respectively.

Figure S2. Correlations between GFP and RFP concentrations. Concentrations of GFP and RFP were measured in the presence of different concentrations of Dox: (a) 16.7 nM, (b) 22.5 nM, (c) 33.7 nM (d), 45 nM and (e) 113 nM. The correlation coefficients between GFP and RFP concentrations are shown at the bottom left of each panel.

Figure S3. Incoherent component isolated from fluctuating protein concentration. (a) Distribution of the incoherent component, z, in the presence of Dox at various concentrations (inset). (b) Standard deviations calculated from the relative distributions. (c) Coefficient b determined from the standard deviation by fitting equation (S22). The average value of coefficient b is 0.016 (a.u.).

Figure S4. Intrinsic noise estimated by correlation analysis. Applying the coefficient b to equation (S18) provided the magnitude of the intrinsic noise at different Dox concentrations (closed circles). The dynamics of intrinsic noise (broken line) was derived using the average of b, which was consistent with that derived using gated cells, as shown in figure 7.

Figure S5. Fluctuation in GFP concentration of restrictively gated cells. A restrictively narrow gate generated a cell population of a specific volume (a). Fluctuation in GFP concentration of gated cells was plotted against the mean ((b), grey circles). Extrinsic noise persists despite the gate region being narrow. The other circles are replots of figure 3(b).

Figure S6. Fluctuation in RFP concentration compared with average GFP concentration. The fluctuation in RFP concentration, i.e. the *CV* of the steady-state distribution, was constant (closed squares) regardless of GFP concentration, and was of the same magnitude as that in GFP concentration (closed circles). A similar result was obtained for gated cells (open circles and open squares).

Figure S1

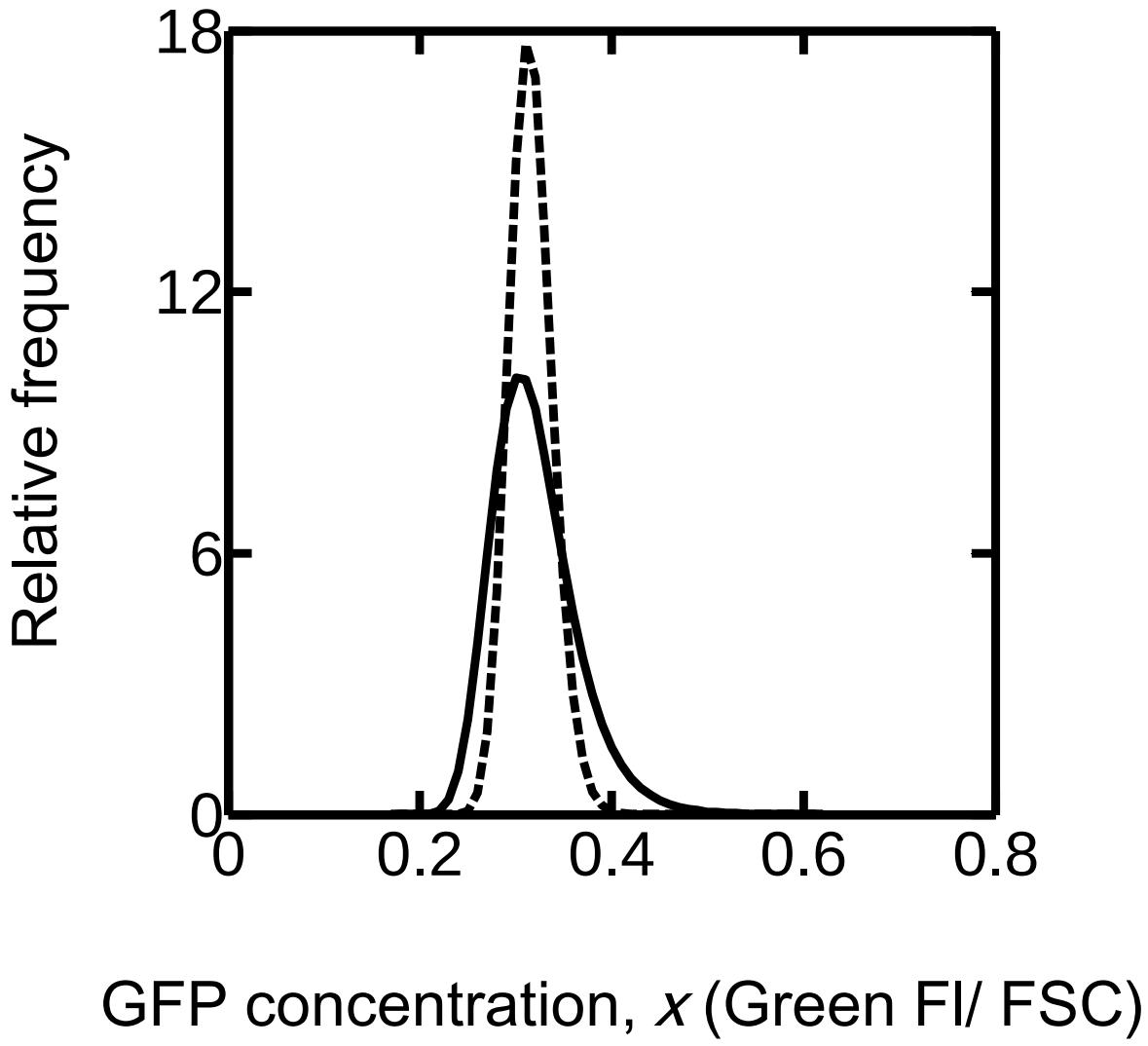
18
12
6
0
Relative frequency
0
0.2
0.4
0.6
0.8
GFP concentration, x (Green Fl/ FSC)

Figure S2

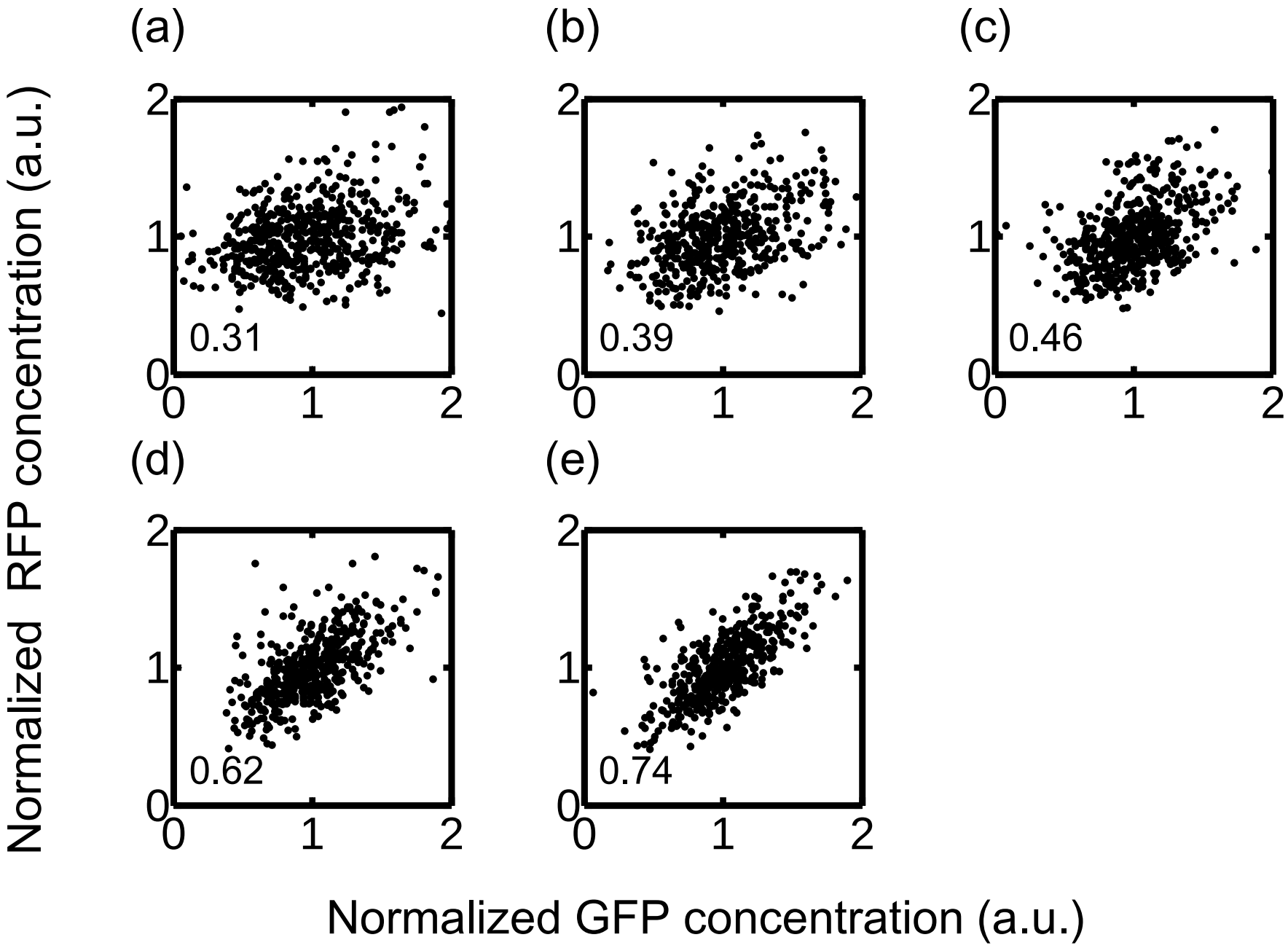
(a)
(b)
(c)
(d)
(e)
0.31
0.39
0.46
0.62
0.74
0
1
2
Normalized RFP concentration (a.u.)
Normalized GFP concentration (a.u.)

Figure S3

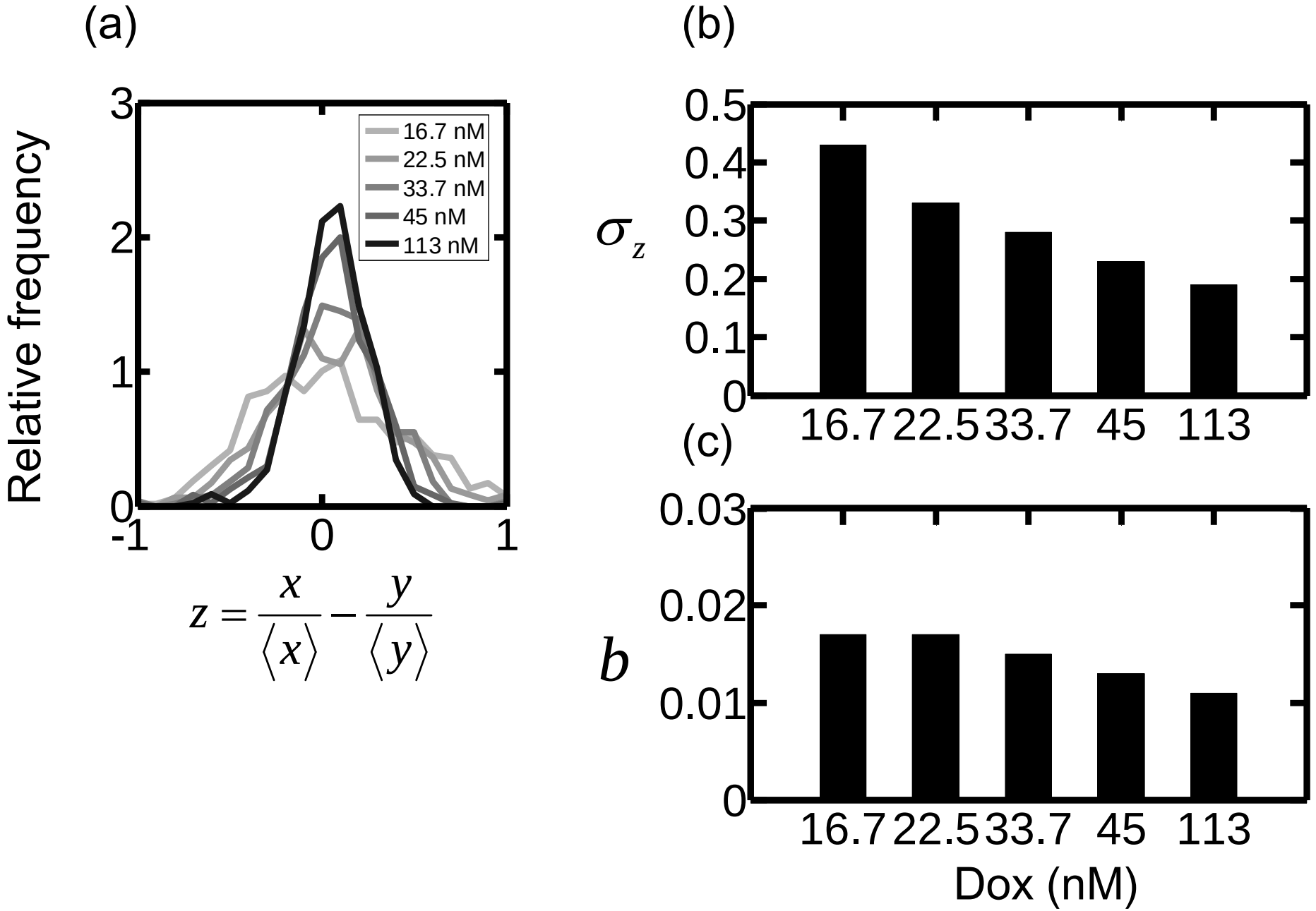
(a)
Relative frequency
16.7 nM
22.5 nM
33.7 nM
45 nM
113 nM
3
2
1
0
-1
0
1
$z = \frac{x}{\langle x \rangle} - \frac{y}{\langle y \rangle}$
(b)
σ_z
0.5
0.4
0.3
0.2
0.1
0
16.7 22.5 33.7 45 113
(c)
b
0.03
0.02
0.01
0
16.7 22.5 33.7 45 113
Dox (nM)

Figure S4

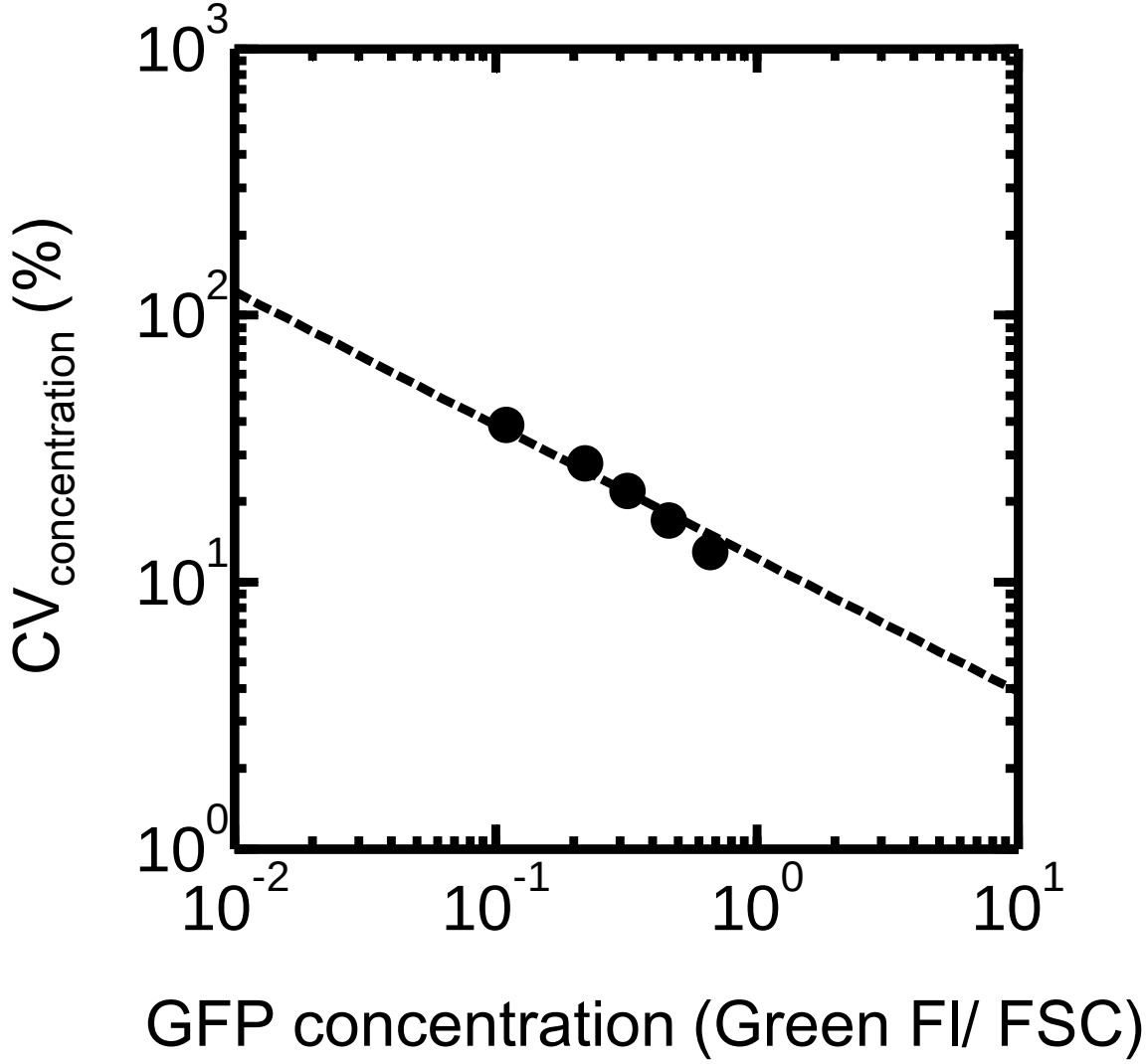
10^3
10^2
10^1
10^0
$CV_{concentration}$ (%)
10^{-2}
10^{-1}
10^0
10^1
GFP concentration (Green Fl/ FSC)

Figure S5

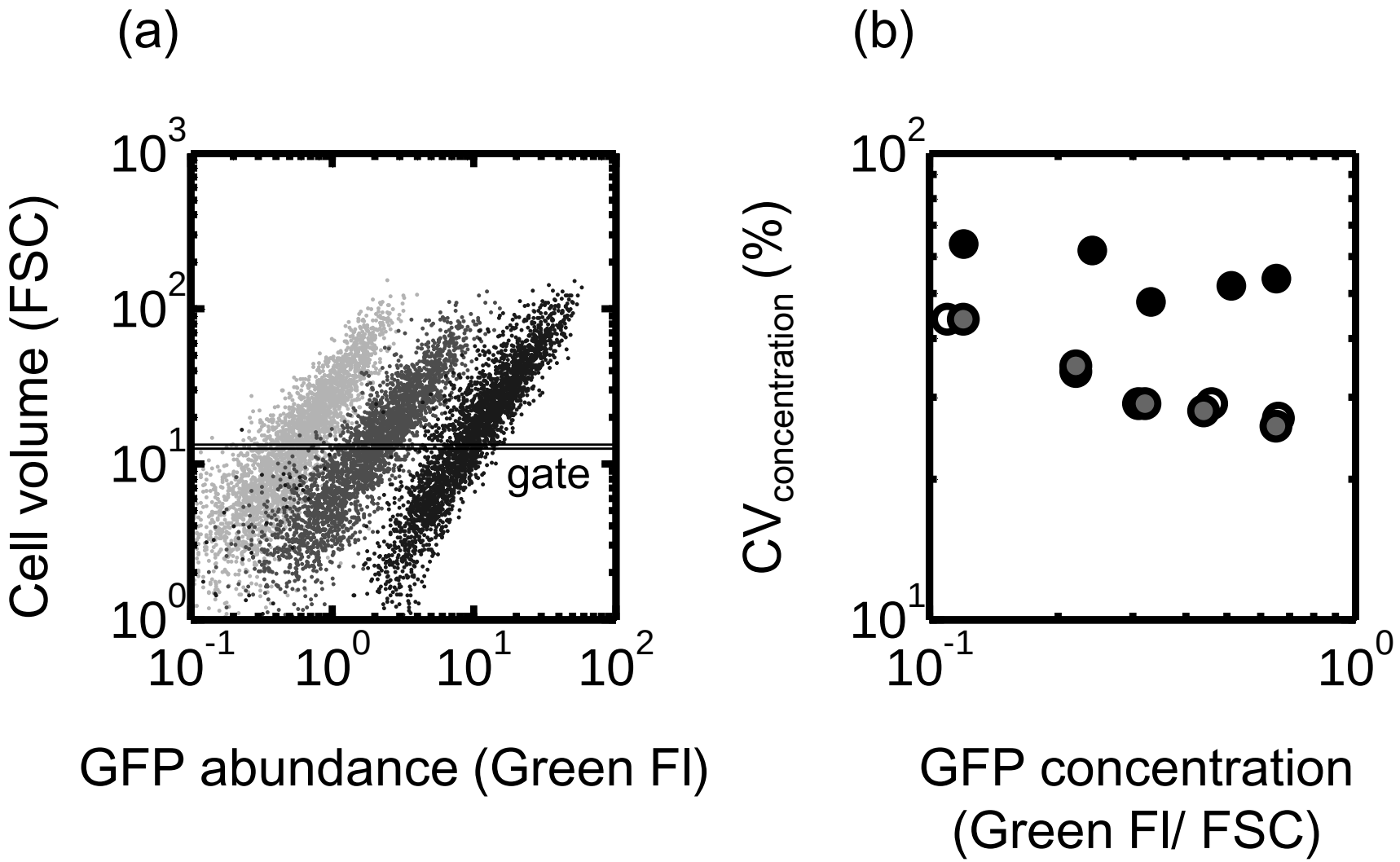
(a)
(b)
Cell volume (FSC)
GFP abundance (Green Fl)
gate
$CV_{concentration}$ (%)
GFP concentration
(Green Fl/ FSC)

Figure S6

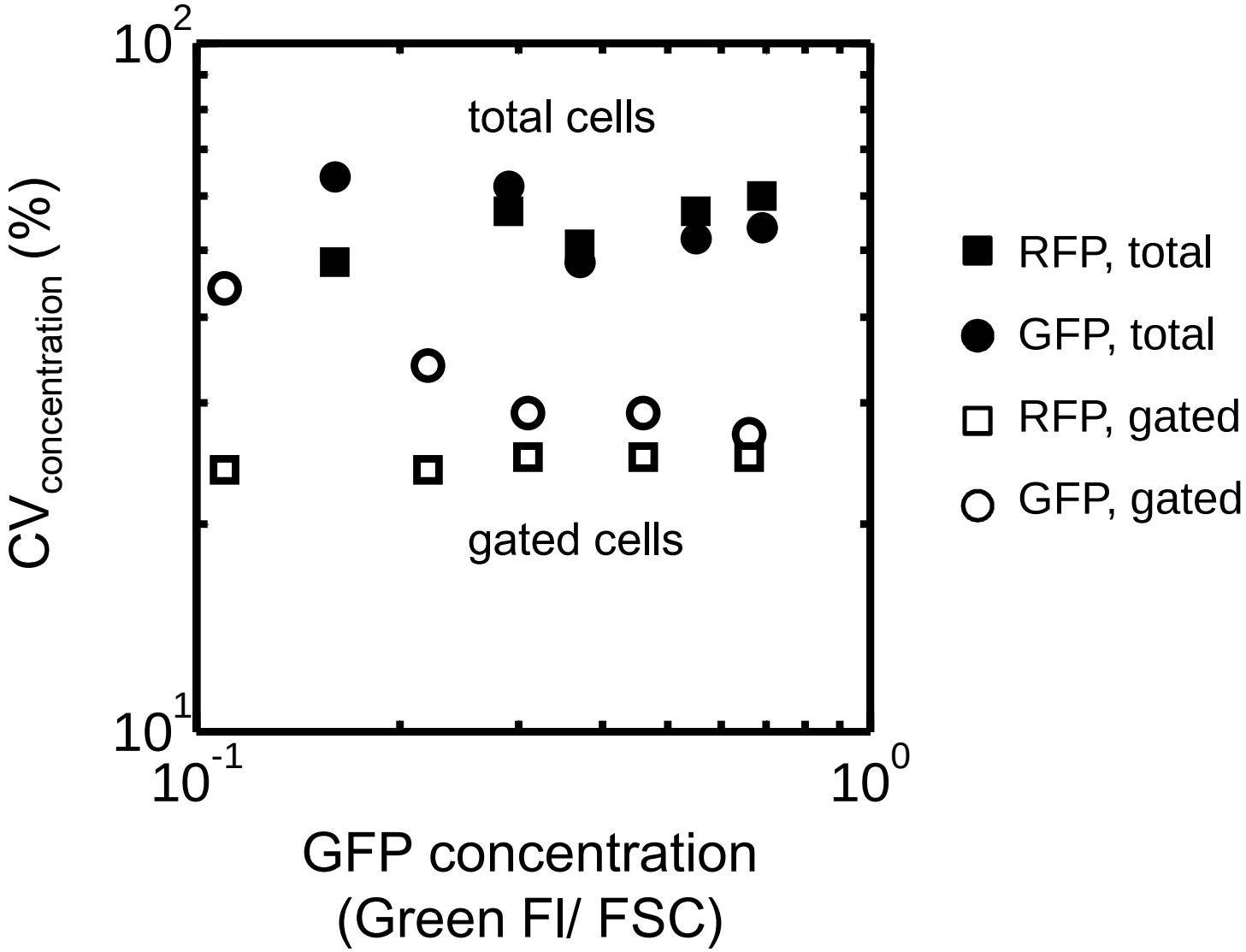
10^2
10^1
10^{-1}
10^0
total cells
gated cells
$CV_{concentration}$ (%)
GFP concentration
(Green FI/ FSC)
RFP, total
GFP, total
RFP, gated
GFP, gated